minerals

MDPI

Article

Soft Roof Failure Mechanism and Supporting Method for Gob-Side Entry Retaining

Hongyun Yang [1,2], Shugang Cao [1,2,*], Yong Li [1,2], Chuanmeng Sun [1,2,3] and Ping Guo [4]

Received: 12 May 2015 ; Accepted: 20 October 2015 ; Published: 28 October 2015
Academic Editor: Saiied Aminossadati

1 State Key Laboratory of Coal Mine Disaster Dynamics and Control, Chongqing University, Chongqing 400044, China; yanghy@cqu.edu.cn (H.Y.); yong.li@unibo.it (Y.L.); sun.c.m@cqu.edu.cn (C.S.)
2 College of Resources and Environmental Science, Chongqing University, Chongqing 400044, China
3 School of Computer Science and Control Engineering, North University of China, Taiyuan 030051, China
4 National Key Laboratory of Gas Disaster Detecting, Preventing and Emergency Controlling, China Coal Technology Engineering Group Chongqing Research Institute, Chongqing 400037, China; aguoping@cqu.edu.cn
* Correspondence: shugang.cao@cqu.edu.cn; Tel./Fax: +86-23-6511-1706

Abstract: To study the soft roof failure mechanism and the supporting method for a gateway in a gently inclined coal seam with a dip angle of 16° kept for gob-side entry retaining, and through the methodology of field investigation and numerical and analytical modeling, this paper analyzed the stress evolution law of roof strata at the working face end and determined that the sharp horizontal stress unloading phenomenon along the coal wall side did not appear after the working face advanced. Conversely, the horizontal stress along the gob side instantly decreased and the tensile stress produced, and the vertical stress in the central part of the roof had a higher reduction magnitude as well. An in-depth study indicates that the soft roof of the working face end subsided and seriously separated due to the effect of the front abutment pressure and the roof hanging length above the gob line, as well as certain other factors, including the rapid unloading of the lateral stress, tension and shear on the lower roof rock layer and dynamic disturbance. Those influencing factors also led to rapid crack propagation on a large scale and serious fracturing in the soft roof of the working face end. However, in the gob stress stabilized zone, the soft roof in the gob-side entry retaining has a shearing failure along the filling wall inside affected by the overburden pressure, rock bulking pressure, and roof gravity. To maintain the roof integrity, decrease the roof deformation, and enable the control of the working face end soft roof and the stabilization of the gob-side entry retaining roof, this study suggests that the preferred bolt installation angle for the soft roof situation is 70° based on the rock bolt extrusion strengthening theory.

Keywords: gob-side entry retaining; unloading loose; bolt installation angle; extrusion strengthening

1. Introduction

The retaining of the gob-side entry is to maintain the head entry of current mining panel behind the working face to be reused for the next panel as the tail entry. This technology can effectively increase the coal recovery rate, reduce the roadway development rate, and mitigate the outburst risk, as no pillar is needed for the retained entry, but rather an artificial filling wall is constructed on the gob side with a special support for entry stability [1].

Since the 1950s, pillarless roadways have been constructed worldwide, and extensive studies have been carried out on support resistance [2,3]. Previous studies showed that the gateway roof rock mass failure mechanism and supporting methods have a significant impact on gob-side entry

retaining, determining the procedure's success. Many researchers categorized five failure types of a gateway roof rock mass, including the compressive stress failure type, tensile stress failure type, shear stress failure type, squeezing and fluidity failure type, and geological structure failure type [4–6]. Based on the above failure mechanism of gateway roof strata, many active support models were suggested, and a combined supporting technology using a bolt, mesh, and cable was found to be effective for ground control. It was found that a combined support is unable to control the main roof in roadway retaining according to the theory of "given deformation", but it can stabilize the immediate roof with the main roof to maintain the retained gob-side entry very well [7,8].

Rock bolts have become a popular technique for reinforcing rock masses all over the world. Rock bolts are installed to reinforce a fractured rock mass by resisting dilation or shear movement along the fractures. Nemcik *et al.* [9] determined that the non-linear bond-slip relationship used in the FLAC model for bolting accurately matches the experimental data reported by Ma *et al.* [10]. Yang [11] divided the anchored force evolution process into three stages and found that a surface structure-like bearing plate produces a maximum anchorage force acting directly on the surface of rock that can provide the greatest degree of support. This not only improved the rock mass stress state but also increased the thickness of the reinforcement structure formed by the anchoring force. Zheng and Zhang [12] determined the shear stress and pressure stress distribution equation for the anchored segment and upon studying the stress distribution rule of anchored segment, found that the effect of the pre-tensioned bolt in the soft rock was superior to that in hard rock. Cao [13] showed that the integrity of the supporting system that prevents local failure of surrounding rock from progressing into overall failure is important in rock bolting, so that reinforcing measures should be taken when necessary. Fan [14] designed a roadway heterogeneity controlling technology on a siltstone roof. Hua [15] made use of bolt support and anchor cable reinforcement support technologies inside and beside a retained roadway, respectively, and maintained the retained gob-side entry very well. Yan [16] used pre-tensioned bolts on a roadway roof with medium and fine-grained sandstones by an extrusion lockset to limit its vertical deformation for entry integrity and also analyzed the mechanical mechanism, technical principle and technical characteristics of bolt and cable coupling supports at a mine site. Chen and Bai [17] used bolts with high pre-tensioning, high strength, and a large elongation rate and cables as the basic supporting element, a single hydraulic prop with a metal hinge top beam as a reinforcement support inside the roadway, and a high-water rapid-solidifying material to support the side of the roadway to effectively control the roof rock deformation with medium and fine-grained sandstones in gob-side entry retaining.

In the past experimental studies and supporting theory [4,14–17], the bolt support is mainly aimed at the control of the medium-hard roof rock mass, which are generally medium and fine-grained sandstones in the horizontal and flat seams. The supporting theory also provides supporting references for the similar conditions of the roadway in the initial excavation stage and retaining stage. However, the working face end roof and retained roadway roof seriously deformed in the soft roof rock mass and gentle inclined coal seam with a soft roof rock after referencing the existed supporting theory. Therefore, to further develop our understanding of the soft roof failure mechanism and provide a supporting method, the following works were conducted in this article. First, the roof failure phenomenon of a gently inclined coal seam working face end and retained roadway were investigated at a coal mine in the southwest of China. Second, the roof failure mechanism was analyzed through the field investigation and stress evolution law obtained by three-dimensional distinct element code (3DEC). Finally, a roof support was designed based on results of this investigation to maintain roadway stability.

2. Description of Field Observation

2.1. Survey of Study Site

The target coal mine is located in the southwest of China. The mining coal seam is #C19, with an average dip angle of 16° and a mining thickness of 1.1 m. The mining method is the fully mechanized

longwall, and gob side entry retaining is used, as shown in Figure 1a. The investigated head entry is buried at 315 m, with a cross-section of 3.8 m in width and 2.1 m in height of the short rib, where resin-anchored rock bolts (Φ20 × 2200 mm), cables (Φ12.54 × 6300 mm), and reinforcement mesh were used, and three rows of single hydraulic supports with top hinged beams were used as advanced strengthening support, as shown in Figure 1b. The roof rock bolts are non-fully anchored (anchor length is 1.4 m) with a pre-tension of 90 kN, inter-row spacing of 800 × 800 mm and bolt angles of 90°, 80°, 70°, and 60° for different bolts, and the extra cables have a pre-tension of 200 kN and an inter-row spacing of 3200 × 1200 mm.

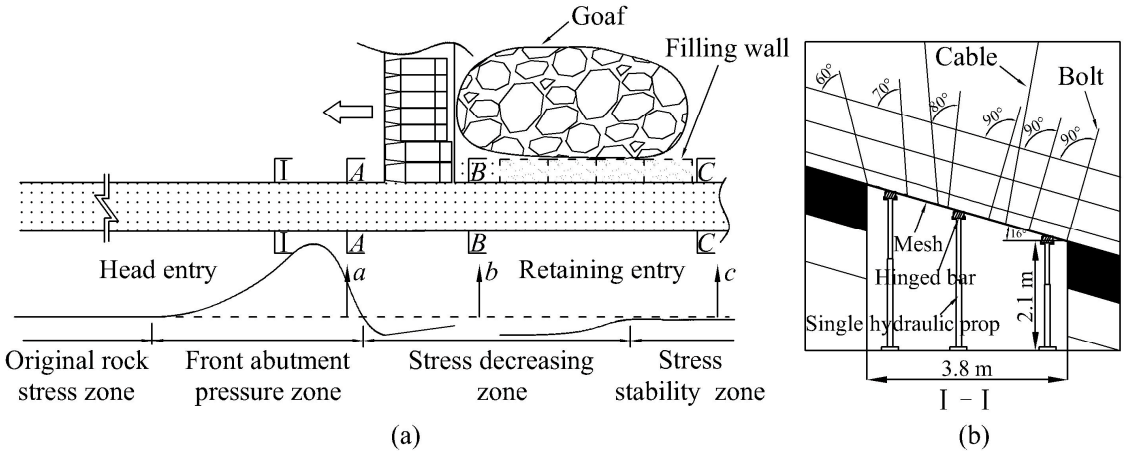

Figure 1. (**a**) Schematic of gob-side entry retaining; (**b**) Schematic of advanced strengthening support.

According to a geological survey, the gateway roof strata typically consist of weak rocks. The immediate roof is approximately 1.0 m in thickness and is made up of sandy mudstone and mudstone. The main roof consists of more competent siltstones and silty mudstones containing siderite nodules. In other words, the roof strata have low strength and poor stability and exhibit clear stratification, thus resulting in an immediate roof caving with the working face advancing as well as part of the main roof. Also, the floor is made up of sandy mudstone. It must be stressed that, at the working face end, the gateway soft roof was often affected by dynamic loading for the following reasons: (1) caving of the overburden rock mass in the gob roof, and the gangue movement, collision; (2) periodic weighting of the main roof; and (3) blasting operations of adjacent mining and excavating faces.

2.2. The Survey Results of Soft Roof Failure Characteristics

The soft roof failure characteristics of the front abutment pressure zone, the stress decreasing zone, and the stress stability zone are shown in Figure 2. According to a filed investigation of the head entry, there was a serious roof deformation due to the impact of front abutment pressure and a few cracks with less opening over a small area of the roof surface, as shown in Figure 2a. With the working face advancing, the roof overhanging length increased, and cracks formed and joined together in the roof rock mass, as shown in Figure 2b, resulting in a decrease of the roof strength, loss of self-bearing capacity, separation from the main roof, and roof deformation and becoming unload rock body, especially for the rock mass indicated by the red line. In addition, two bolts and one cable (B1, B2 and C1) on the gob side lost their support ability. After building the filling wall and removing the supports in the stress stability zone, the roof fractured along the inside of the filling wall, indicated as the "fracture line" in Figure 2c.

Field observations found that there were a large number of cracks in the vertical direction of roof near the end of the working face, so the roof caving occurred generally within a height range of 1.5 to 2 m, as shown in Figure 3.

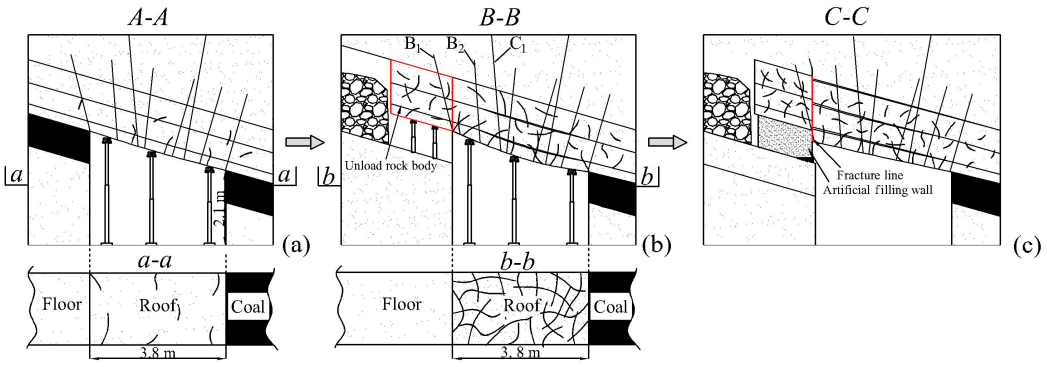

Figure 2. Schematic of soft roof rock mass failure; (**a**) In front abutment pressure zone; (**b**) In working face end; (**c**) In stress stability zone of retaining gateway.

Figure 3. Caving roof near the working face end.

3. Stress Evolution Law in Roof

To analyze the stress evolution law in the roof, the numerical modeling was adopted.

3.1. Numerical Simulation Model

Because of the coal seam condition and as the rock mass was discontinuous [18,19], 3DEC of ITASCA (Minneapolis, MN, USA) [20,21] was used to study the stress evolution law in the roof. The hexahedral model has a length, width, and height of 230 m, 100 m, and 200 m, respectively, includes coal seams and rock strata, with a total of 14 layers, as shown in Figure 4, in accordance with the geological conditions of the investigated mine. The Mohr-Coulomb yield criterion for the materials and the Coulomb slip model for contact were used. The mechanical and physical properties of all the layers and the contacts between every two layers are described in [13,22], respectively.

According to the reference [23], the minimum coefficient of lateral pressure is very close to 0 and the maximum can be up to 6 due to tectonic movement. For this case, we consider the coefficient of lateral pressure is 0.5, as the gateway is placed at shallow depth and close to the anticline axis and seam outcrop, which resulting in a much low horizontal stress. So, the state of the *in situ* stresses is $\sigma_x = \sigma_y = 4.25$ MPa and $\sigma_z = 8.5$ MPa, with σ_y parallel to the longwall advance direction and σ_x perpendicular, as shown in Figure 4b. A vertical pressure of 8.5 MPa is applied on the top surface, and the velocity of the bottom surface was restricted in all three directions, $v_x = v_y = v_z = 0$ m/s. The velocity of the other four surfaces were restricted in the normal direction $v_n = 0$ m/s.

The shape and size of the head entry are introduced in Section 2.1. After an initial equilibrium calculation, rock bolts were installed, as shown in Figure 1b, once the head was entry excavated. The rock bolts were represented as built-in "cable" elements. For resin-grouted rock bolts, the stiffness (K_{bond}) and the cohesive strength (S_{bond}) of the grout are the two key properties that govern the anchor characteristics [22]; $K_{\text{bond}} = 3.06 \times 10^9$ N/m/m and $S_{\text{bond}} = 2.3 \times 10^5$ kN/m were adopted in this study. In addition, a cross-sectional area of 3.142×10^{-4} m^2, an elastic modulus of 200 GPa, and

a tensile yield strength of 165 kN were assigned to the "cable" element. A stepwise excavation in the *y*-direction was adopted to simulate the working face advancing by deleting blocks in five steps of 10 m each, as shown in Figure 4c.

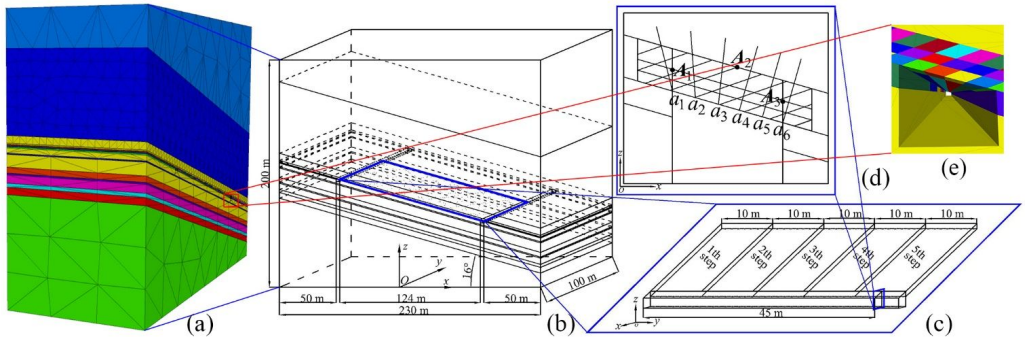

Figure 4. (**a**) Numerical model; (**b**) Coal seam mining model; (**c**) Working face advancing; (**d**) Immediate roof grid, bolt and monitoring points; (**e**) Gateway cross section of model.

3.2. Numerical Results

To understand the stress evolution law, the horizontal stresses in the *x*-direction of points A_1 and A_3 and the vertical stress of point A_2 in the roof at y = 45 m, as shown in Figure 4d, were monitored during the working face advancing, and the results are shown in Figure 5. Especially, it can be found that from A to B Zone, the horizontal stress on the coal side (A_3) increases slightly in magnitude and then reduces to approximately 5.9 MPa, while the horizontal stress on the gob side (A_1) drops instantaneously and appears tensile, and the vertical stress at the gateway central (A_2) reduces significantly to 4.5 MPa as soon as the working face advances beyond the monitor points. The stresses in the gateway roof changed over the whole process from the beginning of the caving to the roof stabilization, until a tensile state was reached, which will influence the stability of the gob-side entry retaining.

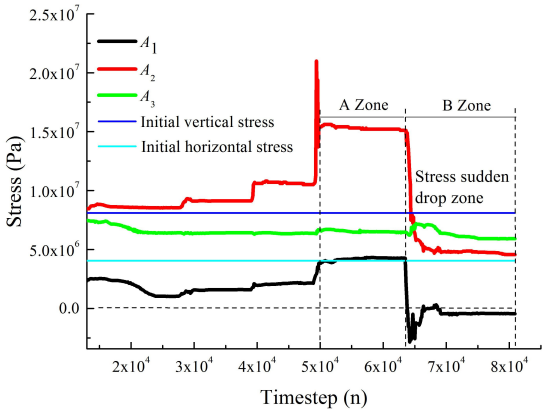

Figure 5. Roof rock mass stress evolution law in working face end.

4. Force States of Roof Rock Mass

Here, combining with the numerical results and field investigation results, the force states of roof rock mass was analyzed to facilitate the failure mechanism analysis of roof rock mass and later theoretical analysis of supporting.

The stress evolution law showed in Figure 5 experienced the front abutment pressure zone (section *A-A* in Figure 1) and stress decreasing zone (section *B-B* in Figure 1). In section *A-A*, there are lateral forces F_{1a} and F_{1b} parallel to the rock strata and an overburden pressure P_1 resembling the

stress (A_1, A_2 and A_3) in A Zone in Figure 5. In addition, field investigation showed that, there are bolt, mesh, and cable support force T_1, reinforced supporting force R_1 in advance, shear forces Q_{1a}, Q_{1b} on the two sides and gravity G. The force state was shown in Figure 6a.

In section *B-B*, the gob side lateral force disappears along the strata strike direction resembling the stress (A_1) in B Zone in Figure 5, because of the roof rock mass caving near the gob side and part of the roof rock mass fracturing, but the coal side lateral force is F_{2b} resembling the stress (A_3) in B Zone in Figure 5. On the other hand, the overburden of pressure is assumed to become 0 resembling the stress (A_2) in B Zone in Figure 5, due to the roof separating from main roof. There are also a bolt, mesh, and cable support force T_2, a strengthen support force R_2 at the working face end and a shear force Q_{2b} in field, also the gravity G. The force state was shown in Figure 6b.

Furthermore, the roof rock mass stress in cross section *C-C* (in Figure 1) has experienced the stress states of sections *A-A* and *B-B*, but, field investigation showed that it will change after the construction of the artificial filling wall and the main roof rotary sinking, and the lateral force F_a on the coal side and the overburden pressure P will restore, the lateral force on the gob side will change to F_b. In addition, the bolt, mesh and cable support force become to T, the shear forces at the two ends become to Q_{1a} and Q_{1b} and gravity remain the same G. The force state was shown in Figure 6c.

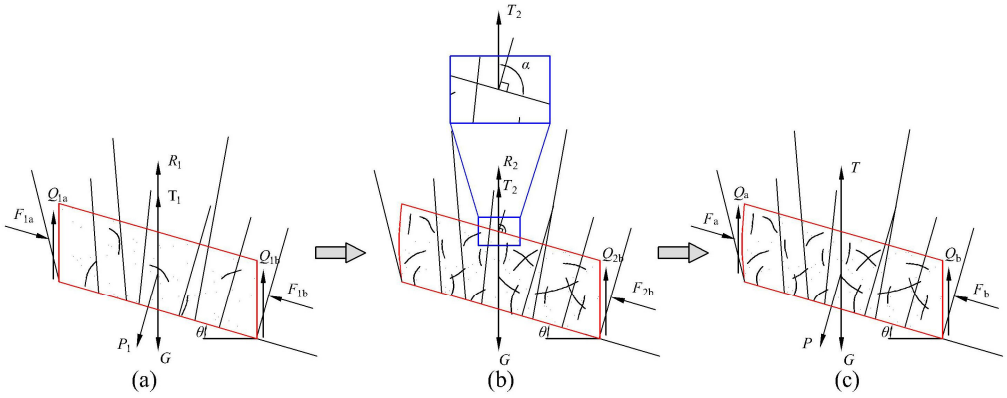

Figure 6. Roof rock mass force; (**a**) Force of cross section *A-A*; (**b**) Force of cross section *B-B*; (**c**) Force of cross section *C-C*.

5. Mechanism for Failure of Roof Rock Mass

Roof failure was affected by many factors, so we will combine them with the failure characteristics obtained by filed investigation, stress evolution law obtained by numerical modeling and the force states to study the roof failure mechanism.

5.1. Mechanism for Failure of Roof Rock Mass in Working Face End

5.1.1. Unloading Effect of the Lateral Stress

Affected by the abutment pressure in the mining and excavation process, the roof rock mass is in the yield state, as shown in cross section *A-A* in Figure 1. The pre-tensioned bolt-cable-mesh supporting system improved the strength, significantly increased the yield strength, and altered the deformation characteristics of the roof rock mass. At the same time, the support system exerted a pressure stress on the rock mass, so the compressive zone stress state had to be altered, which can offset some of the tensile stress and friction and enhance the shear capacity. In addition, the axial and lateral anchored forces increased the shear strength of the weak structural plane, preventing the roof rock mass from moving and sliding along the block structure plane. The pre-tensioned support system controlled the expansion deformation and destruction, preventing roof separation, sliding, fracture opening, and new crack generation in the anchorage zones, not only maintaining the integrity but also forming a pre-tensioned bearing structure with a large stiffness [24,25].

Influenced by the rotary sinking of the overlying roof and the superposition of the overburden pressure, the vertical displacement of the anchor bolt and cable increased significantly, leading to an increase of T_1. The stress increment of the roadway roof rock mass mainly comes from the bulking deformation. When the bolt, mesh, and cable apply pressure on the broken rock mass and adds an anchoring force, the rock mass volume or volume rise rate decrease, and a bulking force is produced by the broken rock mass that would work the bolts and surrounding rock at the same time and put the roof rock mass in an extrusion state. As shown in cross section *A*-*A* in Figure 1, it is precisely because of the interaction of the "support-surrounding rock", that the roof rock mass presented a failure state in Figure 2a.

Although the single hydraulic props support the roof strata with pressure, the extrusion state rock mass above the hydraulic support started loosening on the working face end. In cross section *B*-*B* in Figure 1, the loosening roof rock mass caved behind the support body on the gob side, causing a sharp reduction of the lateral pressure, especially for the accumulated bulking force. Meanwhile, the overburden pressure decreased almost to 0 due to the separation of the soft roof from the hard roof above.

It can be observed that, accompanied by the gob roof caving, the lateral pressure unloaded and the bulking force decreased in the broken rock mass of the roadway roof, leading to its stress state changing from a three-dimensional stress state to a two-dimensional or uniaxial stress state, leading more easily to failure. At this point, together with the tensile stress effect, the rock mass volume "elastic" expansion in the layer strike direction caused the generation and propagation of a large number of cracks and the further failure of the rock mass.

5.1.2. Tensile and Shear Failure of the Working Face End Lower Layer Rock Mass

Through the field investigation of the roof support body layout and its work process and based on the features of the roof rock mass deformation and failure, it is found that the working face end soft roof presents the following phenomenon:

(1) An uneven supporting at the working face end roof. A strong mine ground pressure appeared, causing the significant sinking of the working face end roof in the working face advancing process, so a single hydraulic prop with an articulated roof beam was usually set as a reinforcement support. There is uneven pressure on the roof surface due to the low strength and stiffness of the sandy mudstone and mudstone and the higher strength and stiffness strengthening the support body, resulting in part of the support body inserting the roof and leading to a roof rock shear failure with shear stress q, as shown in Figure 7. In addition, the passive supporting force is too large and does not couple support with the bolts (cables), causing part of the bolts (cables) to be loosened, affecting the roof rock mass local stress state and resulting in ultimate rock mass failure.

(2) Effect of local moment. Treating the reinforcement body (individual hydraulic prop and articulated roof beam, *etc.*) as the fulcrum, the lower roof strata produced a local bending on a small scale, but when the fulcrum bending moment (M) is too large, the layered roof strata cause tensile and compressive damage to the upper surface and lower surface, respectively, additionally increased the possibility of the support body inserting the upper roof and leading to rock mass shear failure, as shown in Figure 7.

The two phenomena above are shown in the Figure 1 *A*-*A* and *B*-*B* cross sections and may occur simultaneously.

5.1.3. Dynamic Failure

The working face end roof rock mass is often affected by vibration as described above. Here, 3DEC was also applied to study the dynamic failure characteristics of the roof rock mass, the coal and rock mass physical and mechanical parameters and the boundary conditions used in the

numerical model shown in Figure 4, additionally adding the model viscous boundary conditions for all boundaries to make the stress wave propagate or be absorbed to simulate the infinite foundation environment. However, we alter the length to 1.6 m in the y direction and treat it as a plane strain model. As the location in cross section *A*-*A* in Figure 1, under the action of a triangle stress wave to simulate the influence of a dynamic disturbance to the roof rock mass. In the simulation process, the stress peak value of the triangle stress wave is 8 MPa rise time is 1 ms and the decrease time is 7 ms [26–29]. Roof bolt (like a_1, a_2, a_3, a_4, a_5, a_6 in Figure 4c) end displacement and the surrounding rock plastic zone were monitored, and the results are shown in Figures 8 and 9 respectively.

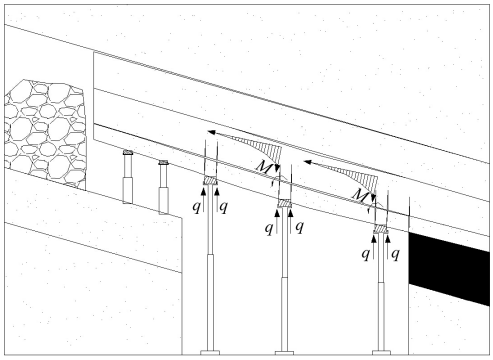

Figure 7. Schematic of support body damage to the roof rock mass.

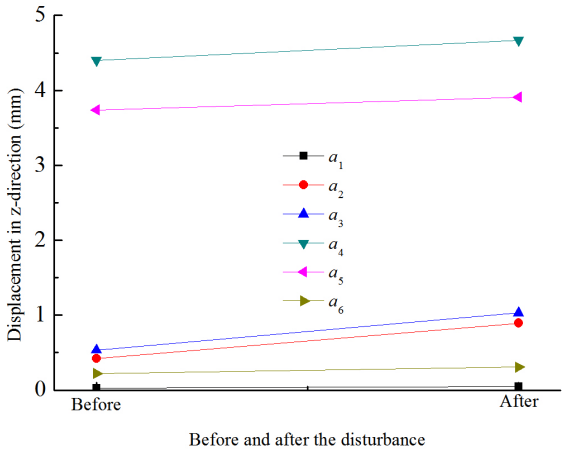

Figure 8. Displacement variation before and after the dynamic disturbance.

Figure 9. Plastic zone of surrounding rock: (**a**) Plastic zone before disturbance; (**b**) Plastic zone after disturbance.

It can be observed from Figure 8 that the displacement of all the monitoring points had a small increase in magnitude after the disturbance.

Figure 9a,b show the plastic distribution zone before and after the dynamic disturbance of the gateway surrounding rock mass, respectively. The stress wave had countless reflections and refractions on the roof crack surface according to the stress wave propagation theory, and the tensile stress would cause changes to the roof rock mass stress state and result in a combination of shear failure on existing joints/weakness horizons, an extension of critically oriented joints and propagation of new fractures through previously intact rock so that the integrity of the roof became poor, the plastic zone expanding into the higher strata, and the ultimate widespread destruction of the roof rock mass [7]. At the same time, the two gateway sides and floor rock mass also produced plastic damage under the stress wave action, but had small extended failure zones.

The above results show that the increment of the displacement and plastic zone was small, but due to the constant increase of the dynamic load, it can be presumed that the working face end soft roof rock deformation and failure magnitude would significantly increase under the repeated dynamic load action, and the more cracks are formed, the more damage caused to the rock mass. To minimize the power damage, there is a need to improve the soft roof rock mass stress state and reduce the development degree of cracks.

5.2. Mechanism for Failure of the Roof Rock Mass in Retaining Roadway

As shown in Figure 2c, cross section *C*-*C* in the stabilized zone in retaining roadway experience a fracture deformation process at the working face end that can be influenced by the main roof rotary deformation and stress recovery process beside the working face, resulting in its larger damage and deformation degree, causing a weakening of its integrity. After strengthening the support of the roof rock mass in the retaining roadway and constructing the artificial filling wall body, their integrity and stability were improved and the bulking force was restored to a certain degree. For a certain retaining distance, after the strengthened support body was recycled, due to the artificial filling wall's higher strength and stiffness, the bulking force would release along its inside. Therefore, the soft roof of retained entry caved at the man-made constructed wall (see shear failure line in Figure 10) due to forces such as the overburden pressure (P), the bulking stress (P_s), rock mass gravity (G) and the bolt, mesh, and cable support force (T), which formed a "similar cantilever beam" structure, as shown in Figure 10.

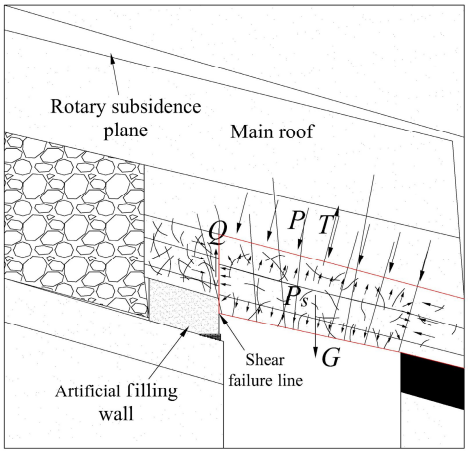

Figure 10. Roof rock mass stress model of the retaining roadway.

6. Roof Support Countermeasures

To develop a supporting method for the roof rock mass at the working face end and retained gateway, the deformation and force in the roof rock mass must be analyzed. The rock bolt is the basic supporting tool. First, we calculated the "cable" element to represent the rock bolts on the working face end with several different bolt installation angles in 3DEC model to find the bolt end

displacement change characteristics. Then, we analyzed the bolt limit equilibrium tension force change features in the retained gateway roof rock mass with the change of the bolt installation angle though the force balance equation.

6.1. Deformation Analysis of Working Face End Roof

From the soft roof failure process and failure characteristics, the following mechanism for the soft roof support can be obtained:

(1) Providing the roof rock mass extrusion stress and changing the rock mass stress state to improve their strength [11]; (2) Preventing cracks from generating and propagating to increase both the strength of the affected roof strata and the stiffness of the whole bolted strata to reduce roof deformation and dynamic damage; and (3) Reducing the broken rock mass bulking force and maintaining the stability of the roadway roof by supporting in time. According to the above points and the "bolt extruding reinforcement theory" by pre-tensioned bolts providing a compressive zone in the axial direction [11], the working face end soft roof mechanical structure should be similar to that in Figure 11 with bolts supporting, so the installation angle is suggested to be $0^\circ < \alpha < 90^\circ$.

The distributed axial stress of the pre-tensioned bolts in the extension direction and the lateral stress vertical axial direction can alter the rock stress state, especially for the thin and weak immediate roof conditions [13]. Here, we use the same numerical model and the physical and mechanical parameters of the rock mass in Figure 4 to analyze the effect of the bolt installation angle α on the stability of the roof rock mass. Bolt installation angles of 50°, 60°, 70°, and 80° (in Figure 12) were applied in the numerical model and the monitoring bolt end displacement was at y = 45 m with the same excavation process as shown in Figure 4 conducted, and the results are shown in Figure 13. As actual field bolt installation at an angle α in the mine roof close to 90°, similar to in Figure 1b, it was taken as 90° to facilitate the analysis, and the results are shown in Section 3.1.

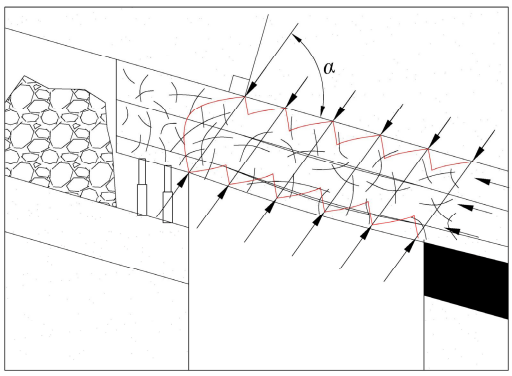

Figure 11. Stress state diagram of soft top supporting effect.

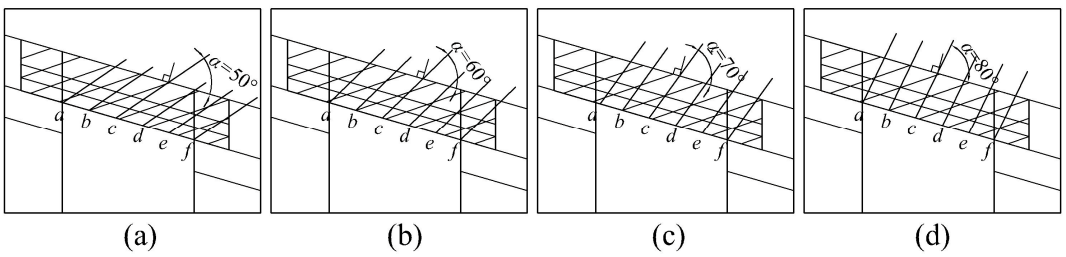

Figure 12. Arrangement diagram of different bolt installation angles: (**a**) 50°; (**b**) 60°; (**c**) 70°; (**d**) 80°.

Figure 13 shows that:

(1) The monitored displacement had a good regularity and the displacement curve showed a trend of a "concave" type with α increasing as a whole; the vertical displacement of roof was

minimal when α = 60°, and the displacement increased when α = 70° and 80°, but it had a smaller increment;

(2) For a certain α, the point displacement increased as the distance to the gob decreased, that is to say, the roof rotated and sank; and

(3) The displacement is larger under the current anchor installation angle (α = 90°) condition; its differences were 155 and 321 mm from the minimum displacement.

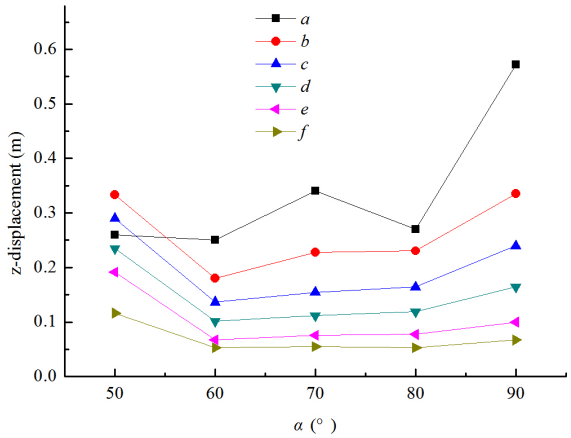

Figure 13. Bolts end displacement.

6.2. Bolt Limit Equilibrium Tension Force

It is known that the working principle of bolts is to maintain the roof rock mass stability in the early stage and to control roof deformation in the later stage. Moreover, carrying out gob-side entry retaining is a systematic project and the roof deformation in the later retaining stage, when maintaining the working face end roof rock mass stability, should be considered. After the construction of the artificial filling wall and recycled reinforcement support body, the roof shear failure (see Figure 2c) is mainly influenced by the bolt-cable-mesh force T, gravity G, shear forces Q_a and Q_b, and the lateral forces F_a and F_b (reference in Figure 6c), regardless of the overburden pressure because of the roof separation, as shown in Figure 14.

At the moment, the roadway roof rock mass undergoes serious failure and its integrity is poor, so it loses its rigid body properties. Therefore, there is distance h_1 between rotating point A and the upper endpoint, so it cannot have a certainty value under the action of torque and $0 \leqslant h_1 \leqslant h$.

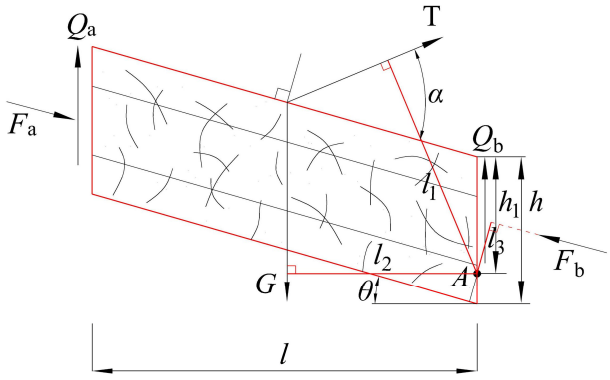

Figure 14. Stresses-Balanced schematic of roof rock mass.

On the other hand, the roof had been cut along the edge of the gob near the artificial filling wall, so the lateral pressure and shear force can be ignored. In the simplified calculation, it can be

set that $F_a = 0$, $Q_a = 0$. The stress balance relationship in the layer strike direction and vertical layer direction are established, as well as the moment balance relationship established by point A, as shown in Equations (1)–(3), respectively.

$$T \sin\alpha + Q_b \cos\theta - G \cos\theta = 0 \tag{1}$$

$$T \cos\alpha + G \sin\theta - Q_b \sin\theta - F_b = 0 \tag{2}$$

$$Tl_1 - Gl_2 - F_b l_3 = 0 \tag{3}$$

where l_1, l_2 and l_3 are the moment arms of T, G and F_b to point A, respectively, as shown in Equation'(4).

$$\begin{cases} l_1 = \sqrt{(h_1 + l/2 \cdot \tan\theta)^2 + l^2/4} \cdot \\ \sin\left[\alpha + \arctan((2h_1 + l\,\tan\theta)/l) - \theta\right] \\ l_2 = l/2 \\ l_3 = (h_1 - h/2)\cos\theta \end{cases} \tag{4}$$

where l is the roadway width 3.8 m, θ is the coal seam dip angle 16°, and the gravity G is calculated according to the following Equation:

$$G = a(n-1)b\,h\,\overline{\rho}\,g\cos\theta \tag{5}$$

where a and b are the bolt inter-row spacing, both 800 mm; n is the number of anchor bolts, 6; h is the study height of the roof rock mass, 1.5 m; $\overline{\rho}$ is the average density of the rock mass, 3000 kg/m^3; and g is the gravitational acceleration, 10 m/s^2.

When $T = 6 \times 90$ kN, G is calculated by Equation (5). Assuming $Q_b = 0$, it can be obtained that $\alpha = 15°$ and 165° according to Equation (1). This means that, if α meets the condition of $15° \leqslant \alpha \leqslant 165°$, the anchor tension force T is greater than or equal to the roof rock mass gravity in the vertical layer direction. Therefore, the roof can remain stable in this direction.

Furthermore, it can be observed from Equation (2) that α impacts the balance relationship of Equation (2) and determines the size of the lateral extrusion force F_b. If $0° < \alpha < 90°$, it can not only satisfy the balance relation but also have a greater F_b value, as does the extrusion stress between the broken roof rock mass in the layer strike direction.

Substituting Equations (2), (4) and (5) into Equation (3) yields:

$$T = \frac{G(l_2 + l_3 \sin\theta) - Q_b l_3 \sin\theta}{l_1 - l_3 \cos\alpha} \tag{6}$$

In reality, the lower roof stratum fails more seriously than the upper rock stratum, indicating that the roof rotating point A is usually above the roof surface. However, as it is impossible to determine the true position of the rotating A, we assume that $h_1 = h$, implying that the rotating point A is at the bottom of study rock body. On the other hand, if the fracture roof rotated, the coal side shear force would decrease more, so we also assume $Q_b = 0$. Then, substituting each parameter of the mine mentioned above into Equation (6), produces:

$$\sin(\alpha + 31.1°) - 0.2584\cos\alpha = \frac{104.12\text{kN}}{T} \tag{7}$$

By analyzing Equation (7), the following results are obtained.

(1) If the T value is small, the right value becomes greater than the left maximum value, so it cannot meet the balance relationship, and the bolts are not able to play their role in supporting. This shows that when having a certain bolt installation angle α, there must be some tensile force T of the bolts to make the right value equal the left value in Equation (7). It also illustrates the importance of the bolts being pre-tensioned when used in the rock mass.

(2) When α takes the values of 50°, 60°, 70°, 80°, and 90°, the relation curve of the bolt tension T under roof rock mass ultimate stability conditions with an installation angle α is shown in Figure 15a, and the change trend is similar to the curve in Figure 12.

Here, it can be explained that when α is kept constant, the smaller the T value, the smaller the force required for the roof rock mass limit equilibrium under the action of the torque; when the actual bolt tension values remain unchanged, the roof rock mass have a minimum displacement, which requires a minimal bolt tension force (T_{min}) for limit equilibrium. For example, in Figure 15a, the largest displacement or the worst stability is when α = 50 and the minimum displacement or the best stability is when α = 70° of the roof rock mass. Hence, the roof displacement is proportional to T.

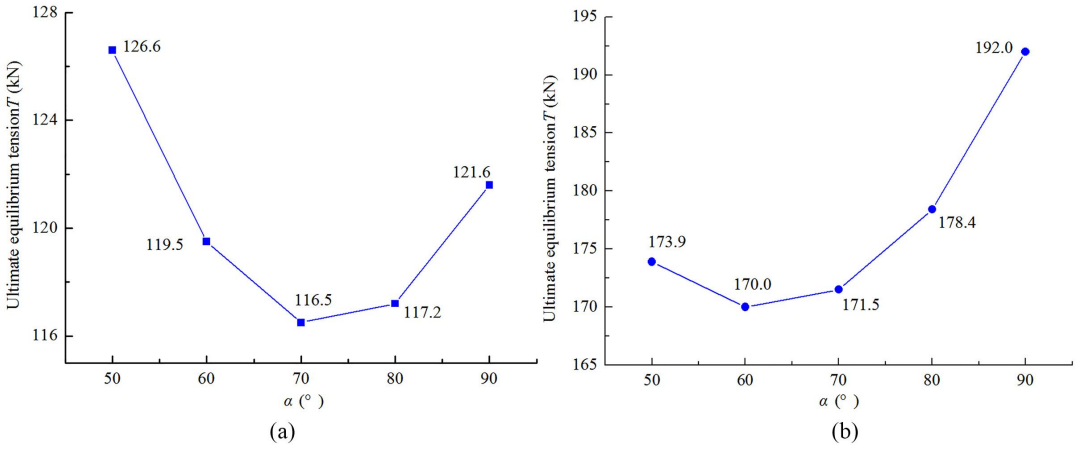

Figure 15. Relationship of limit equilibrium, anchor tension force, and installation angle, (**a**) the study condition when θ = 16°; (**b**) another condition when θ = 0°.

Combining Figures 13 and 15a, it can be observed that when α = 70°, it can provide a failure rock mass with extrusion pressure and alter the stress state, and it can also compress joints and fissures to reduce its opening and the dynamic damage at the same time. Hence, it is advantageous to control the working face end roof and maintain the roof stability in the gob-side entry retaining.

7. Discussion

The thickness of the soft roof stratum in a gently inclined coal seam is small and its strength is low, so mining activities can cause the roof rock mass to serious break and extremely easily cave in, producing a great threat to normal production activities and personnel safety. The selection of a pre-tensioned anchoring technique and bolt arrangement style can improve the bulking roof rock mass stress state by preventing cracks from expanding and reducing the roof separation. To meet the requirements of the retained head entry, a bolt arrangement form is proposed. Furthermore, the application of Equation (6) can be used for the discussion of the supporting measures under similar coal seam geological conditions of, for instance, different coal seam dip angles, gateway widths, and soft roof thicknesses. Because researchers provided more insights into the soft roof failure mechanism of horizontal coal seam by retaining gateway to set α = 90°, thereby assuming the caving height h = 2 m, coal seam dip angle θ = 0°, other conditions remain unchanged as above, thereby determining the proper relationship concerning α and T, as shown in Figure 15b. It shows that T is much large when α = 90° under the high thickness soft roof and horizontal coal seam condition.

On the one hand, the lateral shear forces of Q_a and Q_b in the theoretical calculation process of Equation (7) are not considered here, but the calculation results and the numerical simulation results are very consistent. Hence, it is feasible to treat the theoretical calculation results as a bolt support reference in the field. On the other hand, only the bolts support is mimicked in the numerical

simulation, without incorporating the action of the individual hydraulic props, anchor mesh, and anchor cable, implying that the findings present here are conservative.

In addition, being restricted by current existing technology, it may be difficult to apply this theory practically, as there will be a high degree of drilling difficulty to set the anchor installation angle to $\alpha = 70^{\circ}$ near the gob edge, as recommended by this paper. However, bolts with a theoretical value α can be installed on the coal side, and for the gob side bolts, α can be set as close as possible to the theoretical value so that they will not be influenced by the roof caving in near the gob, as shown in Figure 2, and to make the most use of the bolts resource by improving their force. The point of the roof failure angle decreased as the horizontal stress level increased, indicating that failure tends to occur around the entry corners when the horizontal stress was low [30]. However, the corner bolts (like *e* and *f* in Figure 12) that are installed tilted to the coal side can increase the horizontal stress, so they can prevent shear failure around the entry corners very well.

8. Conclusions

This paper analyzed the roof rock mass failure characteristics and their failure mechanism in the working face end and the gob-side entry retaining, and discussed its support technology according to the special gently inclined seam occurrence conditions. The following conclusions were reached from the analysis process:

(1) After the working face advances, it is found that the horizontal stress of the soft rock mass at the working face end does not exhibit a large magnitude unloading on the coal wall side, but the horizontal stress momentarily fell, and a tensile stress appeared on the gob side. The vertical stress in the gateway central dropped significantly, almost down to zero.

(2) The sinking and separation of the soft roof rock mass in the gently inclined coal seam working face end is affected by the front abutment pressure and the hanging roof on gob side. The initiation and propagation of cracks and the fractures of the rock mass are produced by the actions of the lateral stress unloading loose, tensile, and shear stresses in the low layer caused by uneven support and no coupling support and dynamic disturbances.

(3) The roof rock mass failed in shear mode along the inside of man-made constructed wall in the stability zone of the retained gateway, due to the overburden pressure, bulking force, roof gravity, and combined supporting force. The failed roof forms a "similar cantilever beam" structure.

(4) The equation of the bolt ultimate equilibrium tension force, a function of the seam inclination, gateway width, soft roof thickness, and bolt installation angle, was established according to the stress balance analysis of the roof rock.

(5) To prevent the working face end soft roof rock mass from increasing its deformation and becoming significantly fractured, and also to maintain the gob-side entry retaining roof's stability, it is suggested that the gateway roof bolt installation angle be 70° to provide an extrusion stress, change the rock mass stress state, and improve their strength for better entry maintenance.

Acknowledgments: The authors gratefully acknowledge funding by National Natural Science Foundation Project of China (51474039, 51404046, 51404168, U1361205), Scientific Research Foundation of State Key Laboratory of Coal Mine Disaster Dynamics and Control (2011DA105287–ZD201302, 2011DA105287–MS201403), Fundamental Research Funds for the Central Universities (106112015CDJXY240003), and Program Supported by the Basic Research of Frontier and Application of Chongqing (cstc2015jcy jA90019).

Author Contributions: Hongyun Yang had the original idea for the study and, all co-authors were involved in the analyses work, sample characterization, writing and revising of all parts of the manuscript.

Conflicts of Interest: The authors declare no conflict of interest.

References

1. Yuan, L. *Theory and Practice of Integrated Pillarless Coal Production and Methane Extraction in Multiseams of Low Permeability*; China Coal Industry Publishing: Beijing, China, 2008.
2. Zhang, N.; Yuan, L.; Han, C.L.; Xueb, J.; Kan, J. Stability and Deformation of Surrounding Rock in Pillarless Gob-Side Entry Retaining. *Saf. Sci.* **2012**, *50*, 593–599. [CrossRef]
3. He, T.J. The Breaking Place Prediction of Face End Main Roof Flap Top in the Gob-Side Entry Retaining. *J. China Coal Soc.* **2000**, *25*, 28–31.
4. Zhang, G.H. Roof cracking reason analysis about gob-side entry retaining under initiative support. *J. China Coal Soc.* **2005**, *30*, 429–432.
5. Gou, P.F.; Zhang, Z.P.; Wei, S.J. Physical Simulation Test of Damage Character of Surrounding Rock under Different Levels of the Horizontal Stress. *J. China Coal Soc.* **2009**, *34*, 1328–1332.
6. Coggan, J.; Gao, F.Q.; Stead, D.; Elmo, D. Numerical Modelling of the Effects of Weak Immediate Roof Lithology on Coal Mine Roadway Stability. *Int. J. Coal Geol.* **2012**, *90*, 100–109. [CrossRef]
7. Zhang, D.S.; Mao, X.B.; Ma, W.D. Testing study on deformation Features of Surrounding Rocks of Gob-Side Entry Retaining in Fully-Mechanized Coal Face with Top-Coal Caving. *Chin. J. Rock Mech. Eng.* **2002**, *21*, 331–334.
8. Xie, W.B. Influence Factors on Stability of Surrounding Rocks of Gob-Side Entry Retaining in Top-Coal Caving Mining Face. *Chin. J. Rock Mech. Eng.* **2004**, *23*, 3059–3065.
9. Nemcik, J.; Ma, S.Q.; Aziz, N.; Rena, T.; Geng, X. Numerical Modelling of Failure Propagation in Fully Grouted Rock Bolts Subjected to Tensile Load. *Int. J. Rock Mech. Min. Sci.* **2014**, *71*, 293–300. [CrossRef]
10. Ma, S.Q.; Nemcik, J.; Aziz, N. An Analytical Model of Fully Grouted Rock Bolts Subjected to Tensile Load. *Constr. Build Mater.* **2013**, *49*, 519–526.
11. Yang, S.S.; Cao, J.P. Evolution Mechanism of Anchoring Stress and Its Correlation with Anchoring Length. *J. Min. Saf. Eng.* **2010**, *27*, 2–7.
12. Zheng, X.G.; Zhang, N.; Xue, F. Study on Stress Distribution Law in Anchoring Section of Prestressed Bolt. *J. Min. Saf. Eng.* **2012**, *29*, 365–370.
13. Cao, S.G.; Zou, D.J.; Bai, Y.J.; He, P.; Wu, H. Surrounding Rock Control of Mining Roadway in the Thin Coal Seam Group with Short Distance and "Three Soft". *J. Min. Saf. Eng.* **2011**, *28*, 524–529.
14. Fan, K.G.; Jiang, J.Q. Deformation Failure and Non-Harmonious Control Mechanism of Surrounding Rocks of Roadways with Weak Structures. *J. China Univ. Min. Technol.* **2007**, *36*, 54–59.
15. Hua, X.Z.; Ma, J.F.; Xu, T.J. Study on Controlling Mechanism of Surrounding Rocks of Gob-Side Entry with Combination of Roadside Reinforced Cable Supporting and Roadway Bolt Supporting and Its Application. *Chin. J. Rock Mech. Eng.* **2005**, *24*, 2107–2112.
16. Yan, Y.B.; Shi, J.J.; Jiang, Z.J. Application of Anchor Cable with Bolt and Steel Band Coupling Support Technology in Gob-Side Entry Retaining. *J. Min. Saf. Eng.* **2010**, *27*, 273–276.
17. Chen, Y.; Bai, J.B.; Wang, X.Y.; Ma, S.-Q.; Xu, Y.; Bi, T.F. Support Technology Research and Application inside Roadway of Gob-Side Entry Retaining. *J. China Coal Soc.* **2012**, *37*, 903–910.
18. Jing, L.; Stephansson, O. *Fundamentals of Discrete Element Methods for Rock Engineering-Theory and Applications*; Elsevier: Amsterdam, The Amsterdam, 2007.
19. Gao, F.Q.; Stead, D. Discrete Element Modelling of Cutter Roof Failure in Coal Mine Roadways. *Int. J. Coal Geol.* **2013**, *116–117*, 158–171.
20. Cundall, P.A.; Hart, R.D. *Development of Generalized 2–D and 3–D Distinct Element Programs for Modelling Jointed Rock*; US Army Engineering Waterways Experiment Station: Minneapolis, MN, USA, 1985; SL–85–1.
21. Firpo, G.; Salvini, R.; Francioni, M.; Ranjith, P.G. Use of Digital Terrestrial Photogrammetry in Rocky Slope Stability Analysis by Distinct Elements Numerical Methods. *Int. J. Rock Mech. Min. Sci.* **2011**, *48*, 1045–1054. [CrossRef]
22. Gao, F.Q.; Stead, D.; Kang, H.P.; Wu, Y.Z. Discrete Element Modelling of Deformation and Damage of a Roadway Driven along an Unstable Goaf—A Case Study. *Int. J. Coal Geol.* **2014**, *127*, 100–110. [CrossRef]
23. Xie, H.P.; Gao, F.; Ju, Y.; Gao, M.Z.; Zhang, R.; Gao, Y.N.; Liu, J.F.; Xie, L.Z. Quantitative definition and investigation of deep mining. *J. China Coal Soc.* **2015**, *40*, 1–10.
24. Hou, C.J.; Guo, L.S.; Gou, P.F. *Rock Bolting for Coal Roadway*; China University of Mining and Technology Press: Xuzhou, China, 1999; pp. 38–50.

25. Kang, H.P. Study and Application of Complete Rock Bolting Technology to Coal Roadway. *Chin. J. Rock Mech.* **2005**, *24*, 161–166.
26. Zhang, Y.Q.; Peng, S.S. Design Considerations for Tensioned Bolts. In Proceedings of the 21st International Conference on Ground Control in Mining, West Virginia University, Morgantown, WV, USA, 6–8 August 2002; pp. 131–140.
27. Lu, W.B.; Yang, J.H.; Yan, P.; Chen, M.; Zhou, C.; Luo, Y.; Jin, L. Dynamic Response of Rock Mass Induced by the Transient Release of *in-situ* Stress. *Int. J. Rock Mech. Min. Sci.* **2012**, *53*, 129–141.
28. Felice, J.J.; Beattie, T.A.; Spathis, A.T. Face Velocity Measurements Using a Microwave Radar Technique. In Proceedings of the 7th Research Symposium on Explosives and Blasting Technique, Las Vegas, NV, USA, 6–7 February 1991; pp. 71–77.
29. Preece, D.S.; Evans, R.; Richards, A.B. Coupled Explosive Gas Flow and Rock Motion Modeling with Comparison to Bench Blast Field Data. In Proceeding of the 4th International Symposium on Rock Fragmentation by Blasting, Vienna, Austria, 5–8 July 1993; pp. 239–246.
30. Peng, S.S. *Coal Mine Ground Control*, 3rd ed.; China University of Mining and Technology Press: Beijing, China, 2013; pp. 200–203.